Prediction of Vessel Icing for Near-Freezing Sea Temperatures

JAMES E. OVERLAND

Pacific Marine Environmental Laboratory, NOAA, Seattle, Washington

(Manuscript received 27 February 1989, in final form 27 October 1989)

ABSTRACT

The operational NOAA categorical vessel icing algorithm is evaluated with regard to advances in understanding of the icing process and forecasting experience. When sea temperatures are <2–3°C above the saltwater freezing point there is the likelihood of supercooling of the spray during its trajectory and extreme ice accretion on topside structures. The NOAA algorithm shows excellent results when compared to a new cold-water dataset from the Labrador Sea (mean sea temperature of −1.3°C), even though the algorithm was developed from an Alaskan dataset with a mean sea temperature of 3.6°C. A rederived algorithm from the combined dataset is nearly identical to the operational algorithm. The influence of sea temperature in the NOAA model is consistent with the supercooling hypothesis and an additional icing category of extreme is recommended for the algorithm. Severe icing in the Bering Sea, Gulf of Alaska, and Sea of Japan is primarily caused by extreme cold-air advection, while low sea temperatures contribute to severe icing in the Labrador Sea, Denmark Strait, and Barents Sea. Indirect verification showed that NOAA provided excellent forecasts to over 140 fishing vessels in Alaskan waters during late January 1989, the worst icing episode of the decade. This case suggests that current-generation atmospheric models are capable of providing reliable 36-h forecasts of cold-air advection, and thus indicating regions of heavy icing. A wave height/wind speed threshold for the onset of topside icing is 5 m s^{-1} for a 15-m vessel, 10 m s^{-1} for a 50-m trawler and 15 m s^{-1} for a 100-m vessel, developed from seakeeping theory. These wind speeds are exceeded 83%, 47% and 15%, respectively, during February in the Bering Sea.

1. Introduction

Vessel icing, and subsequent loss of stability, is a hindrance for expanded marine operations in high latitudes (Fig. 1). The rate of icing depends on wind speed, air temperature, sea temperature and the characteristics, speed and heading of the vessel. Because the dependence of icing on the three environmental parameters is not a simple linear combination, vessels often depend on weather services for warnings of potential icing (Zakrzewski et al. 1988a). This paper reviews the guidance product for icing forecasts prepared in the United States and the process of vessel icing with regard to sea temperature and vessel length.

Physical processes associated with ice accretion are numerous and complex. Icing processes are traditionally divided into the mass flux, which determines how much water is brought to vessel topside surfaces, and the heat flux, which determines the amount of wave-generated spray accumulated as ice on decks and structures. Wave heights depend on wind speed, the duration that the wind has blown, and the fetch, the water distance over which the wind has acted. As waves become higher, their wavelength and wave period become longer. Because there is actually a distribution of wavelengths, wave energy is represented by an ocean wave spectrum and the magnitude of spectral peak increases as the dominant wave length shifts to long waves. As the dominant wavelength approaches the vessel length, vertical motion is generated between the vessel and the sea. Wave-generated spray is produced by slamming and wave impact onto the ship hull. The amount of spray generated by a vessel depends on the ocean wave field, the vessel length, vessel heading and speed relative to the wave field, and the vessel's seakeeping performance—stability, freeboard and hull shape. Once the spray cloud is produced, the vertical distribution of the cloud is important, and even the size of the droplets is an issue because size determines the rate of cooling of the droplet on its trajectory toward the ship. Once the spray reaches vessel surfaces, continued cooling of the ocean water from its sea temperature to the surface equilibrium temperature is determined by the heat flux away from the surface, a function of local wind speed and air temperature. The actual airflow around a vessel is quite complex. The freezing process itself is complicated because of the influence of ocean salinity, which affects the freezing temperature and contributes to forming a low density "spongy" ice with air and brine pockets (Makkonen 1987). The volume of water that flows back off the vessel is much greater than that which remains accreted as icing, yet cooling applies to the total mass flux. A result of these factors is large variation of icing accumulation with respect to location on the vessel, and from vessel-to-vessel. Accumulation on isolated structures such as cranes can be more than twice as heavy as flat hori-

Corresponding author address: James E. Overland, Pacific Marine Environmental Lab, NOAA Bld. #3, 7600 Sand Point Way NE, Seattle, Washington, 98115-0070.

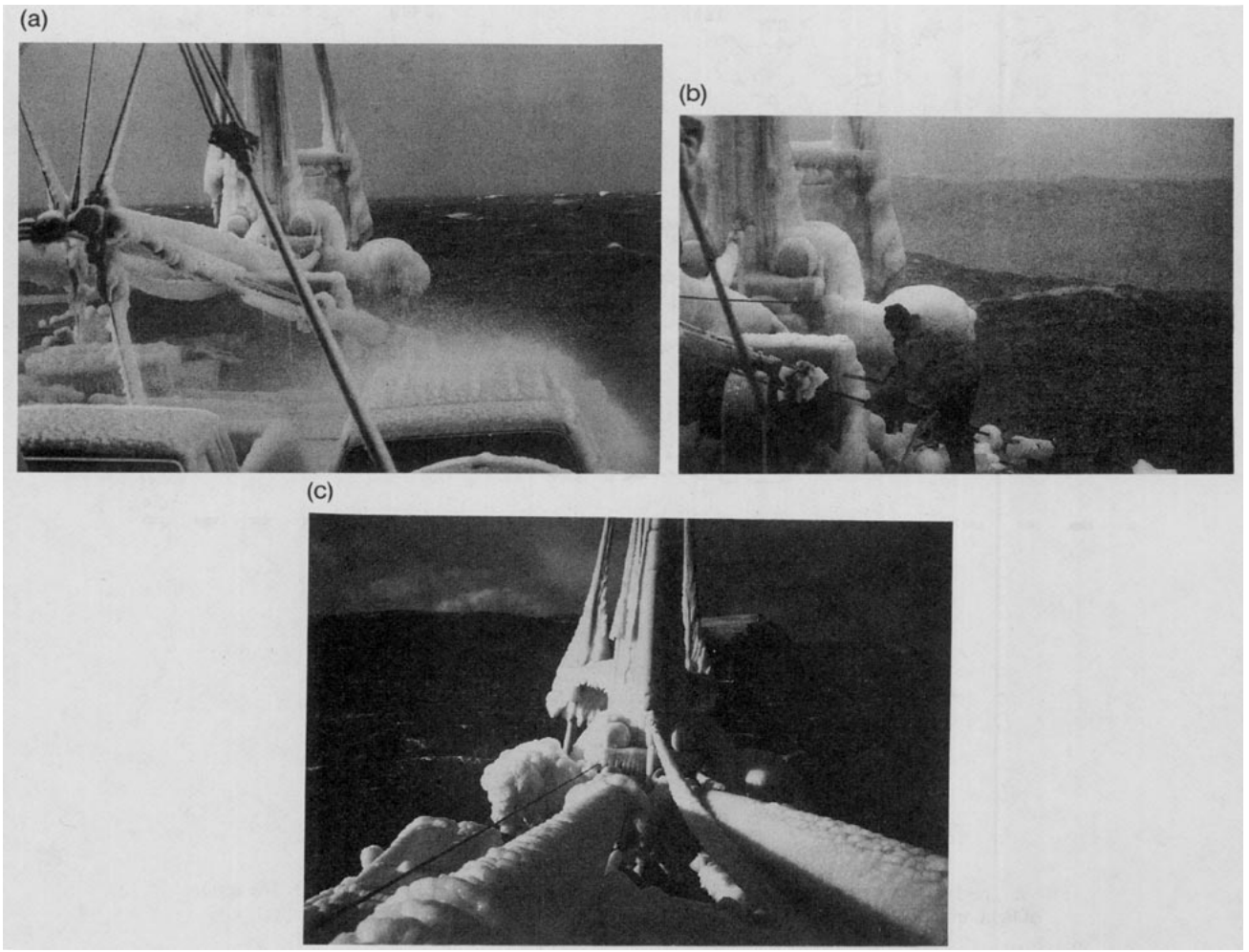

FIG. 1. Moderate icing on the 55-m coastal freighter *Dolphin*, 18–19 February 1982, 56°N, 154°W. (a) The mounds at the beginning of the event are trucks covered with ice. (b) There was 15-cm accumulation over a 24-h period with an intense 6-h period of 22-m s^{-1} wind, −11°C air temperature and 7-m waves. Sea temperature is estimated at 4°C. (c) The vessel was saved by reaching the Semidi Islands along the Alaskan Peninsula. (Photos courtesy Taylor Campbell.)

zontal surfaces (Zahn 1985). Icing rates vary with vessel length, freeboard, and shape, e.g., smaller fishing vessels (≈20 m), coastal freighters and crabbers (≈60 m) to military, ferry, and oceanographic type vessels (>100 m).

A role of weather services is to provide warnings for potential icing conditions and an indication of severity. In a previous paper (Overland et al. 1986, referred to as OPPC) a categorical algorithm was developed for relating icing potential to environmental parameters. OPPC sought to overcome developmental difficulties by careful corroboration of a set of 85 icing observations from Alaskan waters (Pease and Comiskey 1985, hereafter referred to as PC), use of an icing predictor which considered the icing process, and use of a robust statistical procedure which minimized observational difficulties from estimated icing rates and variation between vessels and location on vessels. Rather than a model of icing for a particular place on a particular vessel, the NOAA algorithm sought a balance between model physics, observations, and accuracy of 36–48 h meteorological forecasts, which provide the primary input to the algorithm. The present paper reviews the conclusions of OPPC, without the extensive statistical development, and discusses the implementation of OPPC and recent developments in modeling the icing process.

2. The present algorithm

The NOAA ice accretion chart (Fig. 2) has been produced daily since winter 1986–87 (Feit 1987), based on OPPC. Feit (1987) showed that OPPC was an improvement over previous estimates when compared to independent data from 1986 in the Gulf of Alaska. The chart has three categories of potential icing rate (Table 1 and Fig. 3) with predictor (for notation see Appendix)

$$\mathrm{PR} = \frac{V_a(T_f - T_a)}{1 + 0.4(T_w - T_f)}. \qquad (1)$$

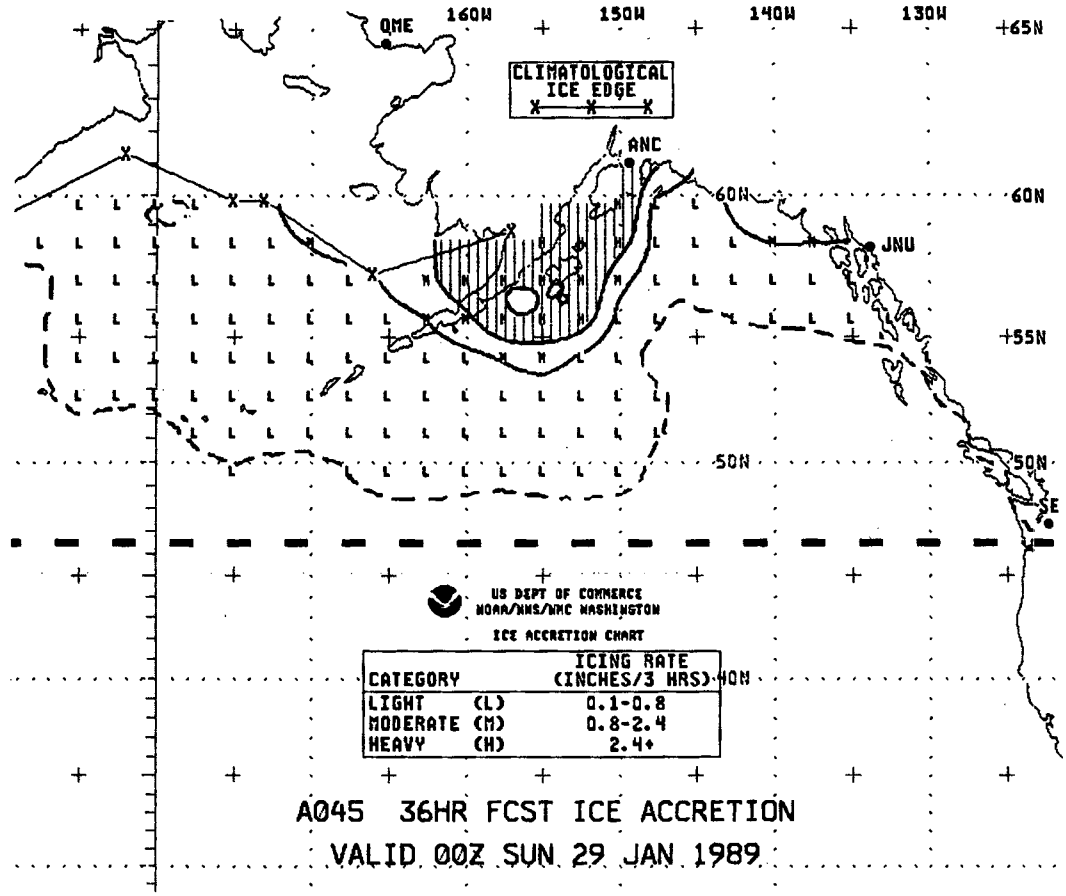

FIG. 2. The 36-h NOAA vessel icing forecast valid for 29 January 1989 (courtesy D. Feit). The regions of light, moderate and heavy icing forecasts are indicated with L, M, and shaded H, respectively.

It was shown in OPPC that the quality of the training data was consistent with an algorithm that was limited to differentiating between no more than three categories of icing. Applying multiple regression to the PC dataset or applying robust techniques to a noncorroborated set of routine ship observations produces no skill (Roebber and Mitten 1987).

TABLE 1. Categorical forecast procedure (Overland et al. 1986).

	Icing class			
	Light	Moderate	Heavy	Extreme (proposed)
Icing rate (cm h^{-1})	<0.7	0.7–2.0	>2.0	
Predictor (PR*) (m°C s^{-1})	<20.6	20.6–45.2	>45.2	>70.0

* $PR = V_a(T_f - T_a)[1 + 0.4(T_w - T_f)]^{-1}$

where

V_a wind speed (m s^{-1})
T_f freezing point of seawater (−1.7°C for North Pacific)
T_a air temperature (°C)
T_w sea temperature (°C)

The coefficient between icing rate and the predictor value, and the coefficient of the sea temperature correction, i.e. 0.4°C^{-1}, were determined from a set of 52 open-ocean observations in Alaskan waters taken when the vessels were not heading downwind (PC). The form of (1) is roughly consistent with a heat balance

$$L_i\rho_i \frac{dH_i}{dt} + C_w(T_w - T_f)\rho_w \frac{dH_w}{dt} \approx C_H\rho_a C_a V_a(T_f - T_a) \quad (2a)$$

which becomes

$$[1 + \Phi(T_w - T_f)] \frac{dH_i}{dt} \sim AV_a(T_f - T_a). \quad (2b)$$

The right-hand side of (2) represents heat transfer, proportional to the product of wind speed and air-temperature depression below the freezing point. The first term on the left-hand side of (2a) is the heat removal required to freeze the water that remains accreted as ice. The second term accounts for the cooling of the seawater to the freezing point for both the water that remains accreted to the surface and runs off the ship.

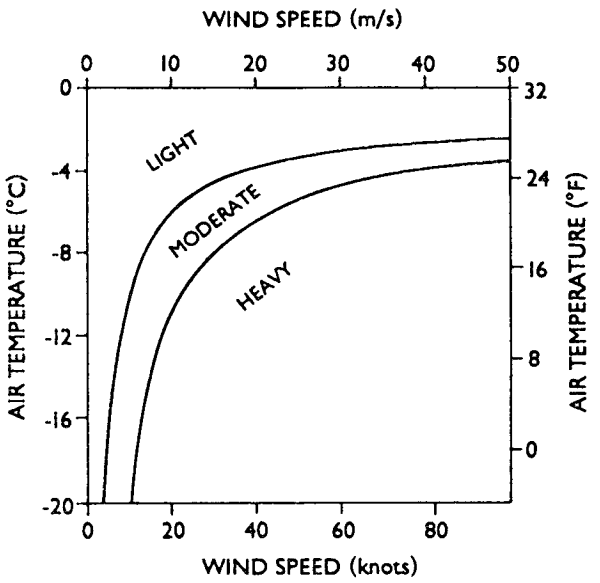

Icing conditions for vessels heading into or abeam of the wind for water temperatures of + 1°C (34°F)

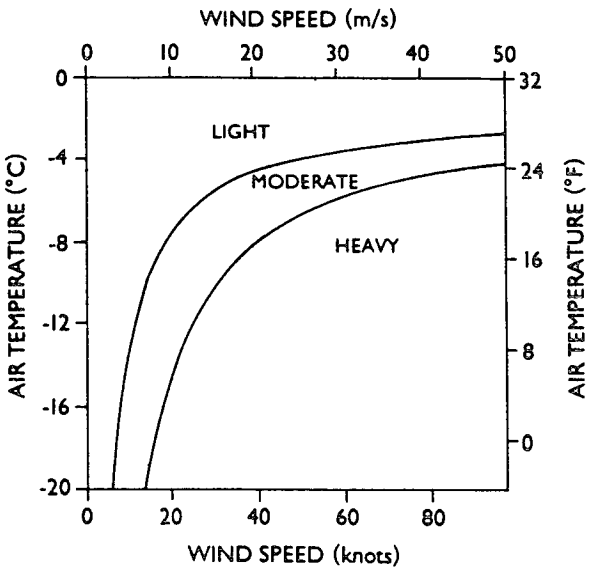

Icing conditions for vessels heading into or abeam of the wind for water temperatures of +3°C (37°F)

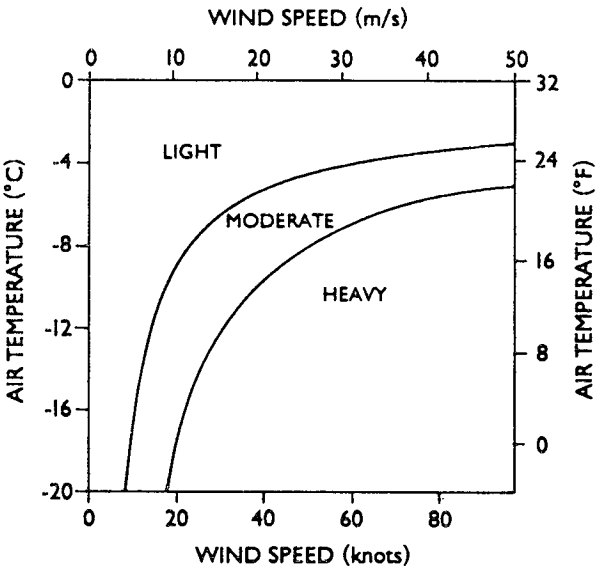

Icing conditions for vessels heading into or abeam of the wind for water temperatures of +5°C (41°F)

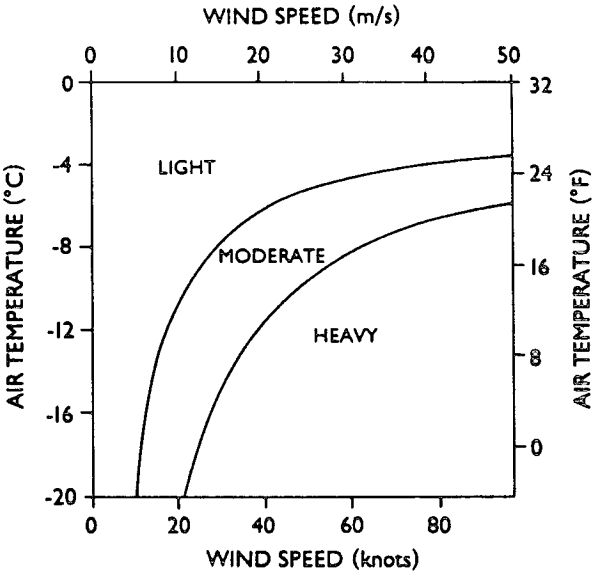

Icing conditions for vessels heading into or abeam of the wind for water temperatures of +7°C (45°F)

Light Icing - Less than 0.7cm/hr (0.3in/hr)
Moderate Icing - 0.7cm/hr (0.3in/hr) to 2.0 cm/hr (0.8in/hr)
Heavy Icing - Greater than 2.0cm/hr (0.8in/hr)

FIG. 3. A plot of the OPPC algorithm for four sea temperatures.

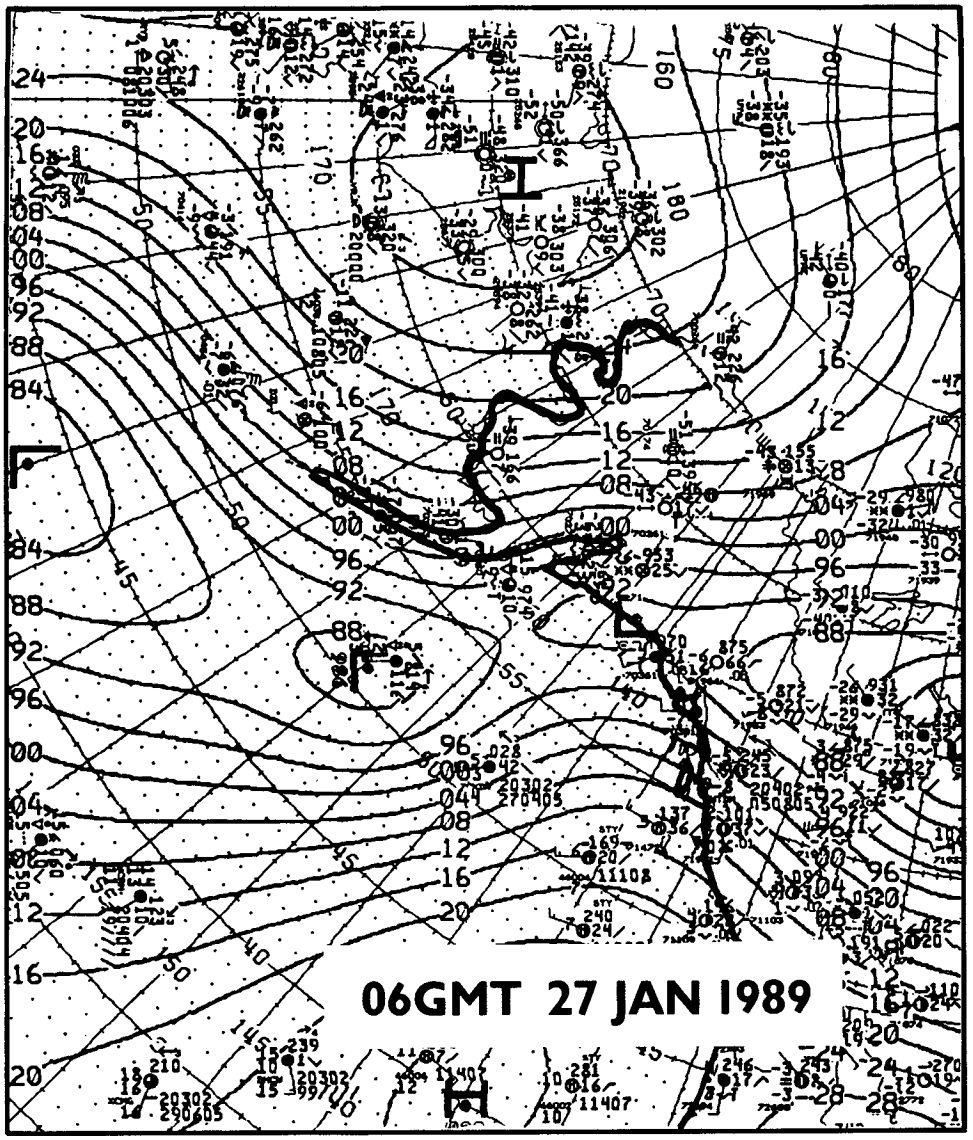

FIG. 4. Sea level pressure analyses from the January 1989 icing event. (a) On 25–27 January, cold air is seen coming from the Arctic Ocean; it continued to cool as it crossed Alaska and exited over the Bering Sea. Coastal-station air temperatures were −39°C. (b) On 29–30 January, the region of strong cold coastal outflow from Alaska had shifted to the Gulf of Alaska.

The cooling of the water which remains accreted is a small effect (Stallabrass 1980), but the total volume of water that is shipped onboard as represented by the inverse of the accretion fraction F can be large, and explains the strong empirical dependence of icing rate on sea temperature (OPPC). Note that OPPC assumes an adequate supply of delivered spray to the deck surfaces, that details of the freezing process do not substantially change the first-order dependence of icing rate on environmental variables given by (1), and that there are no details for specific vessels. Parameters A and Φ, and thus F, vary more slowly as a function of the input variables V_a, T_a, and T_w than the input variables themselves, and thus are assumed constant even though they are certainly weak functions of these input variables. The critique of OPPC by Makkonen (1988, 1989) that F is a function of icing rate is not correct because F is defined as a ratio which is slowly varying.

Input fields for NOAA icing forecasts are 1000 mb air temperature and wind speed from the National Meteorological Center (NMC) spectral forecast model (aviation run; Bonner 1988) and a blended satellite and ship sea-surface temperature analysis (McClain et al. 1985). To locate the contours in Fig. 2 a polynomial was fit to the crossing point between icing categories, the zero crossing, and the median value of icing rate

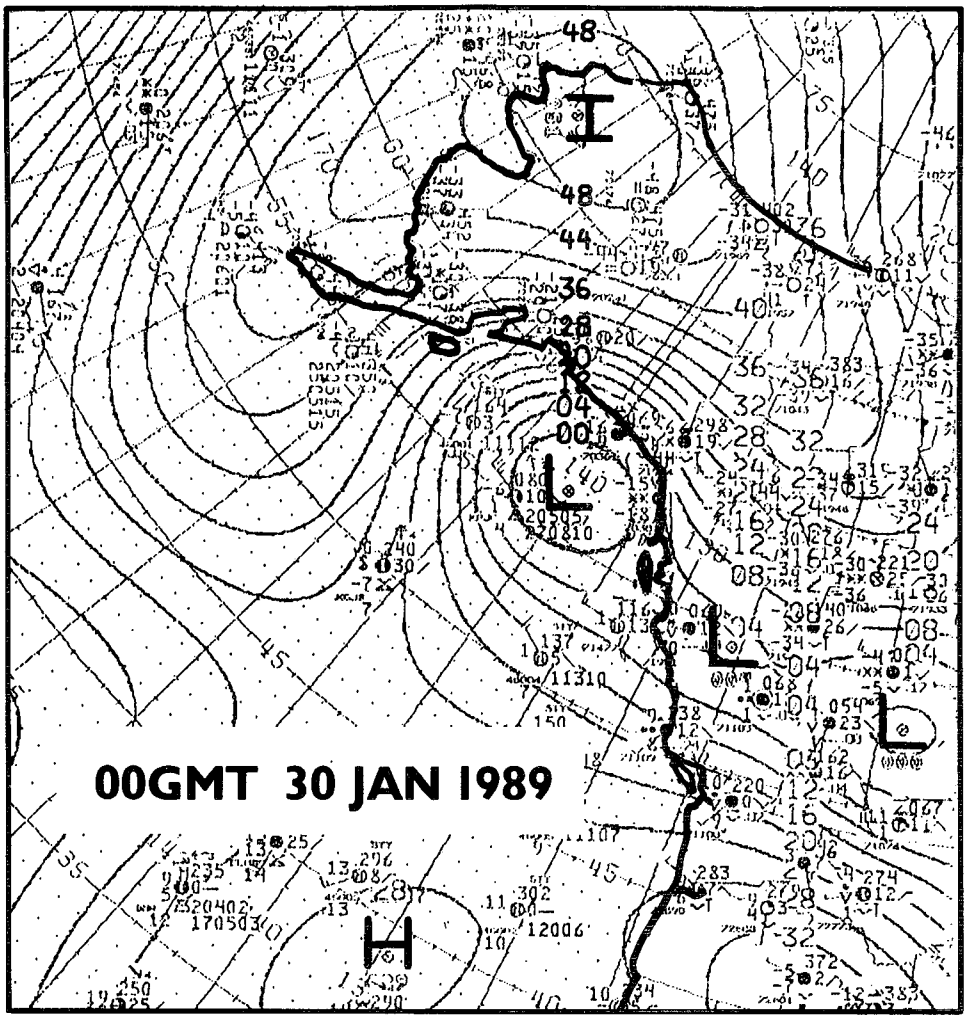

FIG. 4. (*Continued*)

and predictor value for the heavy icing class. The icing rate formula for continuous variables is given by

$$\mathrm{IR(cm\ h^{-1})} = A(\mathrm{PR}) + B(\mathrm{PR})^2 + C(\mathrm{PR})^3 \quad (3)$$

where

$A = 2.73 \times 10^{-2}$,
$B = 2.91 \times 10^{-4}$,
$C = 1.84 \times 10^{-6}$.

Note that the polynomial in (3) has no more skill than is implied by differentiation into the three icing classes in Table 1, especially for large values of the predictor.

3. A western Arctic example from January 1989

Forecasts of vessel icing are dependent on the accuracy of meteorological forecasts of cold-air advection and the reliability of sea-temperature analyses. Direct verification of the NOAA algorithm has not been completed since Feit (1987). However, there is indirect data from January 1989 which had the worst icing potential of the 1980 decade. Severe cold-air advection occurred in late January 1989 over the Bering Sea, and then in the Gulf of Alaska (Fig. 4). During the week of 23–27 January, heavy icing was correctly forecast over the southern Bering Sea. A crab fishing fleet of 140 vessels remained safely in the lee of the Pribilof Islands during the event. Two days later the region of cold-air advection and potential for vessel icing had moved to the Gulf of Alaska. This movement was well forecast by the NOAA model at 36 and 48 h (Fig. 2); the longitudinal extent of heavy icing was particularly well forecast. Unfortunately, a 31-m crabbing vessel, the *Vestfjord,* sank with six crew members, approximately 60–70 miles southwest of Kodiak Island due to vessel icing, just inside the region of forecast heavy icing. Conditions are estimated at 17–20-m $\mathrm{s^{-1}}$ winds, air temperature of $-10°$–$-14°$C, 6-m significant wave

height, and a sea temperature of 3°–4°C, although the vessel estimated 30-m s^{-1} winds and 9-m seas. The vessel probably did not take evasive action early enough. The quality of these icing forecasts, particularly the regional extent, was primarily the result of the quality of the forecasts of wind and air temperature obtained from the NMC Aviation run, which is a 18-layer, 80-wave spectral model.

There were major skill improvements in NMC models in the 1970s with the switch from a grid point to spectral model, and in 1986 advanced physics and high resolution were introduced. Improvements were most noticeable in sea level pressure forecasts; skill of the 48-h forecasts in 1987 was equivalent to the skill of 36-h forecasts in 1986 and to that of 24-h forecasts in 1977 (Bonner 1988). In addition to greater improvement at 1000 mb than 500 mb, there was greater improvement at high latitudes and in winter. Bonner (1988) is validated by the NMC/Fleet Numerical Oceanographic Center/European Centre 48-h forecast evaluation of Alden (1988), who noted good model verification downstream of data sources. Sixty percent to 74% of the difference between persistence and the verifying 500–1000-mb thickness field for April 1988 was forecast by the NMC model for the Bering Sea/Gulf of Alaska, Sea of Japan, Barents Sea, and Labrador Sea. The only potential icing area with lower skill was in the vicinity of Iceland with 41% (Alden 1988, p. 224). Clearly, numerical guidance provided reliable 36–48 h forecasts of persistent cold-air advection during the worst western Arctic icing event of the decade.

Single sea-temperature estimates from satellite may be in error by 1°C due to inexact correction for atmospheric moisture, with errors greater for higher latitudes (Walton 1988). However, persistence and comparison with surface observations probably bring the overall error in sea-temperature analyses to <0.5°C (McClain et al. 1985). This magnitude represents a 6% change in the predictor value at a sea temperature of 3.6°C. With this error magnitude, the icing regions (as in Fig. 2) shift but the pattern and maxima would be unchanged. Because satellite sea temperatures are calibrated against buoy temperatures rather than radiation skin temperatures, they may be more accurate for the purpose of vessel-icing forecasts than for air-sea heat flux.

4. The vessel icing process at low sea temperatures

A concern of OPPC is that (1) may overpredict at low sea temperatures because Φ was fit to the PC Alaskan dataset with a mean sea temperature of 3.6°, compared to the Stallabrass Atlantic dataset mean of 0.7° (Roebber and Mitten 1987). Recent deterministic models (Zakrzewski and Lozowski 1987; Zakrzewski et al., 1988b; Horjen and Carstens 1989) and earlier studies (Stallabrass 1980) suggest that at low sea temperatures (<0°), spray is cooled to supercritical values and becomes a heat sink when it hits the vessel. Supercooled water contributes to rapid ice accretion, while large volume of warm sea-spray continues as a heat source (Fig. 5a and 5b). Supercooling combined with small accretion fractions give the strong qualitative dependence of icing rate on sea temperature as shown in Fig. 5. Ross Brown (personal communication) has indicated that the sensitivity of icing rate to sea temperature may be less in models with time-dependent

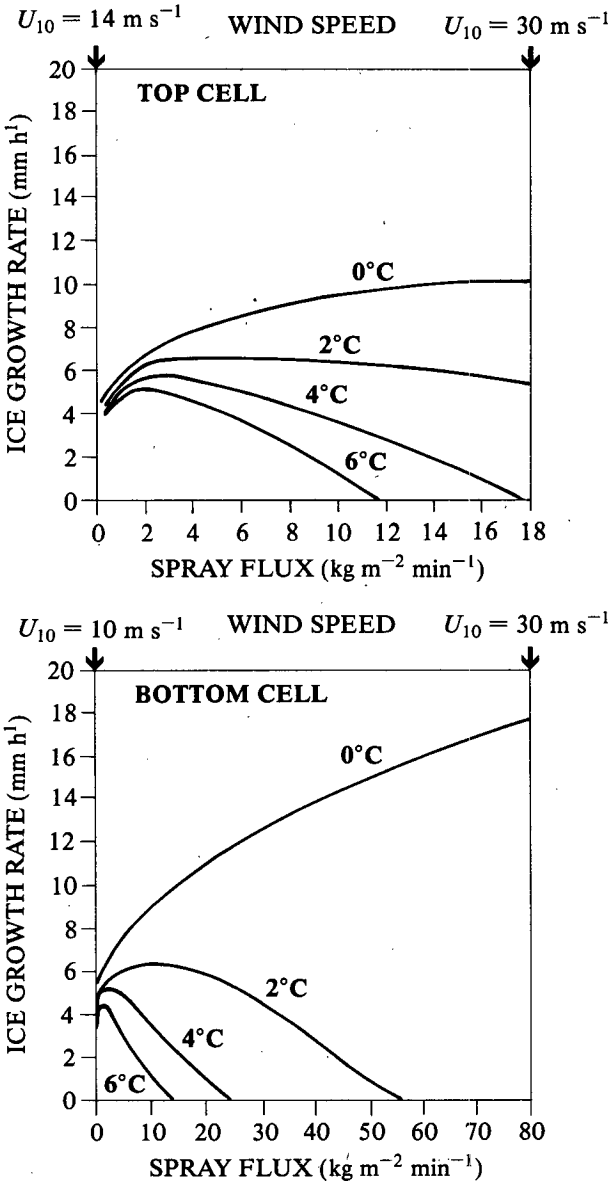

FIG. 5. Modeled spray icing growth rates for the (a) top and (b) bottom of a central column of the ship's superstructure as a function of spray delivery and sea surface temperature (from Zakrzewski et al. 1988b). There is a major dependence of icing rate with sea temperature and location on the vessel.

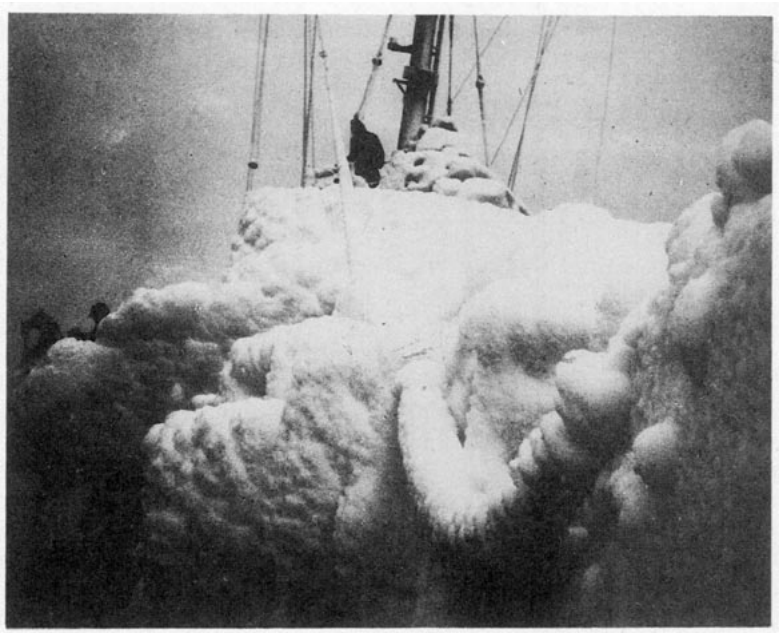

FIG. 6. Up to 25 cm of ice covers USCGC *OWASCO* in the Labrador Sea. (U.S. Coast Guard photo from De Angelis 1974.)

growth rates than models such as Fig. 5 which assume steady growth rates. However, observational support for the existence of extreme icing at low sea temperatures is provided by Lee (1958), De Angelis (1974) and George (1975), who report icing rates in excess of several centimeters per hour near ice edges in the Barents Sea, Labrador Sea, and Denmark Strait (Fig. 6).

Deterministic models for specific cases support the generalized functional form of the denominator in (1) at near-freezing sea temperatures (Fig. 7). OPPC predicts that heavy icing (>2.0 cm h^{-1}) occurs at a moderate wind speed and air-temperature depression for low sea temperatures. To date, extrapolation to more severe meteorological conditions was limited because

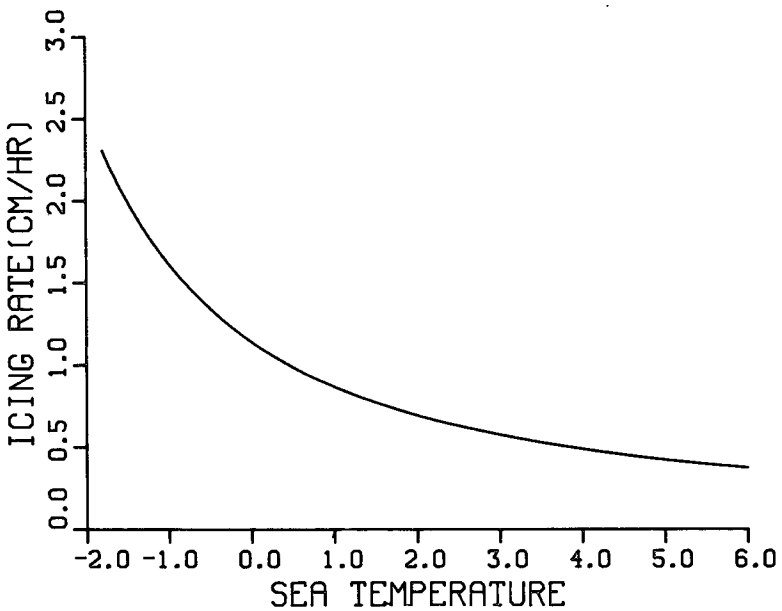

FIG. 7. Dependence of icing rate on sea temperature for a wind speed/air-temperature deficit product of 500-m s^{-1}°C from OPPC. Icing generally does not occur for sea temperatures warmer than 6°C.

TABLE 2. Predicted/observed table for the OPPC icing algorithm applied to a cold sea temperature ($\bar{x} = -1.3°C$) observation set from the Labrador Sea (ZLH). The number of correctly predicted observations is 31% or 70%.

	Observed		
Predicted	L	M	H
Heavy	0	3	9
Moderate	7	11	0
Light	11	3	0

of the few number of extreme icing cases documented in PC at low sea temperatures. However, OPPC argued from photos of vessels that ice accretion in near-freezing water can be significantly >2.0 cm h^{-1} (Fig. 6).

There now exists a cold-water dataset collected by the University of Alberta Group (Zakrzewski et al. 1989, hereafter referred to as ZLH). The 44 ZLH observations were made from a fishing-type vessel in the Labrador Sea during 8–26 February 1988. The mean sea temperature was −1.3°C with many observations at −1.8°C, the freezing point of sea water. The NOAA algorithm evaluated against ZLH has an a_0 score (number correctly assigned observations divided by total number of cases, OPPC) of 0.70 (Table 2), compared with 0.73 on the original PC Alaskan training dataset (52 points). The NOAA algorithm shows skill for the ZLH observations because an a_0 score of 0.70 is greater than the score that could be obtained through chance ($a_{901} = 0.52$). The a_{901} score is obtained by Monte Carlo techniques (see appendix in OPPC). The OPPC algorithm gives reasonable results over the sea temperature range of −1.8° to 6.5°C for moderate-size fishing vessels. Wind and air-temperature depression in the Labrador region may be much greater than those from ZLH and the OPPC threshold values for heavy icing. Therefore, for operations, a fourth icing category—extreme—is recommended for the NOAA algorithm (Table 1) at PR > 70 m s^{-1} °C, even though its absolute rate of icing is uncertain.

For planning, one can anticipate the sea-temperature conditions encountered in different regions of the world. In regions where sea temperatures are <0°C there is the potential for supercooling and extreme ice accretion. One such area is the southern Labrador Sea (Fig. 8) due to the cold, southward flowing coastal current. The range of meteorological parameters for severe icing in this region contrasts with the Gulf of Alaska and central Bering Sea (Fig. 9). In the Bering Sea, northerly winds advect sea ice southward, which melts and cools the ocean. The band of subzero sea temperatures is narrow and the presence of sea ice limits wave fetch. In Alaskan waters severe cold-air advection such as the January 1989 case is required for heavy vessel icing. The Sea of Okhotsk and Sea of Japan are similar

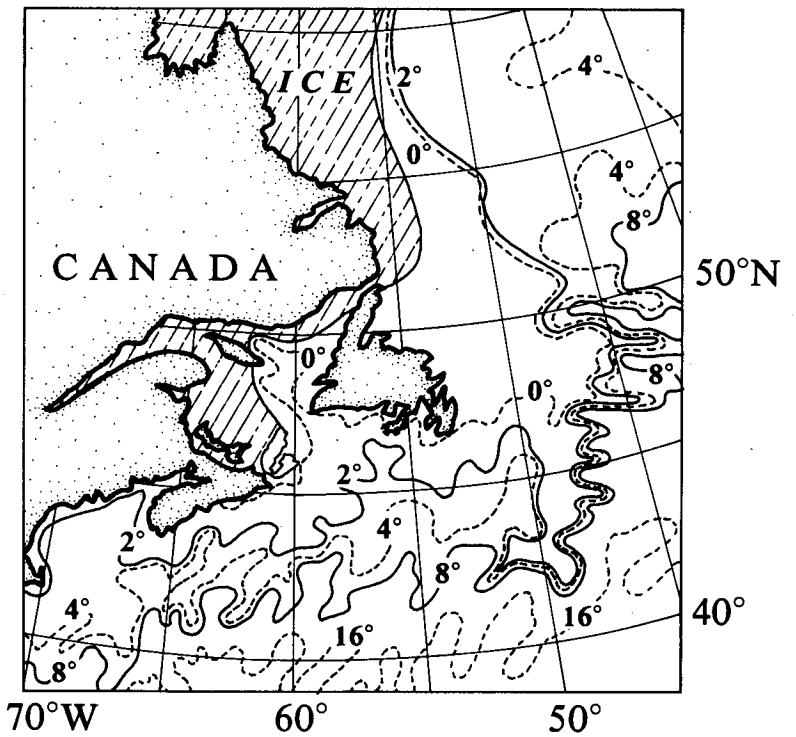

FIG. 8. Sea surface temperatures for 10–16 March 1970, Eastern Canada (Stallabrass 1971). Note the large area of subzero sea temperatures northeast of Newfoundland.

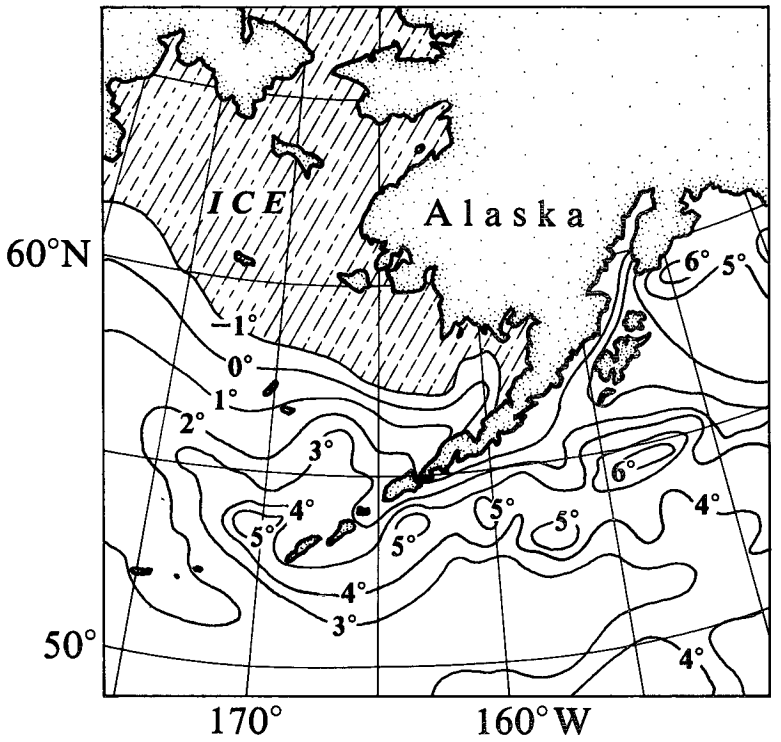

FIG. 9. Sea surface temperatures for 7–9 March 1988, Alaskan waters (Courtesy R. Scheidt). Cold sea temperature occur near the ice edge.

to the Bering Sea (Fig. 10). The western part of the Barents Sea is similar to the Bering Sea; however, a tongue of cold sea-temperatures exists to the east (Fig. 11). For the Denmark Strait northwest of Iceland (Fig. 11) the extent of 0°C water is small, yet icing conditions in this region can be severe (George 1975).

5. Discussion of icing rates

Although OPPC emphasizes categorical forecasts for operations, there is concern that the algorithm may quantitatively overpredict icing rate. To minimize the influence of data from different vessels and vessel operations, OPPC define a potential ice rate as the "maximum sustained rate for typical Alaskan vessels, 20–75 m in length, which are not actively avoiding icing through heading downwind, moving at slow speeds or avoiding open seas." For the purpose of algorithm development, the potential icing rate for each observation from the PC dataset was established as the mean of the maximum reported icing rate and the event rate, the total thickness accumulated divided by the event duration (Fig. 12); several of the maximum reported rates are particularly large. A purpose of OPPC was to point out that potential heavy icing rates were of order 2.0 cm h^{-1}, a rate over five times greater than obtainable with certain earlier forecast aids, most notably Mertins (1968). This disparity is related more to differences in data analysis such as inclusion of downwind cases than real geographic differences in icing conditions.

Because of the OPPC emphasis on potential icing rate, one expects that OPPC rates may be greater compared to other datasets or model calculations. This could be due to differences in sampling location on a vessel, vessel size, using visual estimates or simply changing the procedural definitions of icing. For example, from the PC dataset, the median icing rate from the moderate icing category is 1.7 cm h^{-1}, and the median event rate is 1.0 cm h^{-1}. For heavy icing the median icing rate is 5.1 cm h^{-1}, compared with a median event rate of 2.5 cm h^{-1}. Icing rates of 1–3 cm h^{-1} are not uncommon in case studies of heavy icing (De Angelis 1974) and models (Zakrzewski et al. 1988b).

To test whether inclusion of the maximum icing rate in the original development influenced OPPC, the entire algorithm statistical procedure was rerun using the combined ZLH observations (44) and the PC observations (58). In a first case the icing categories at 0.7 and 2.0 cm h^{-1} and the definition of icing rate as the mean of the maximum and event rate were the same as OPPC (Table 1). In a second case icing categories were set at 0.5 and 1.5 cm h^{-1} and the event rate was used from PC.

For the first case the a_0 score is 0.72 when $\Phi = 0.4$, consistent with the fit for the ZLH observations alone

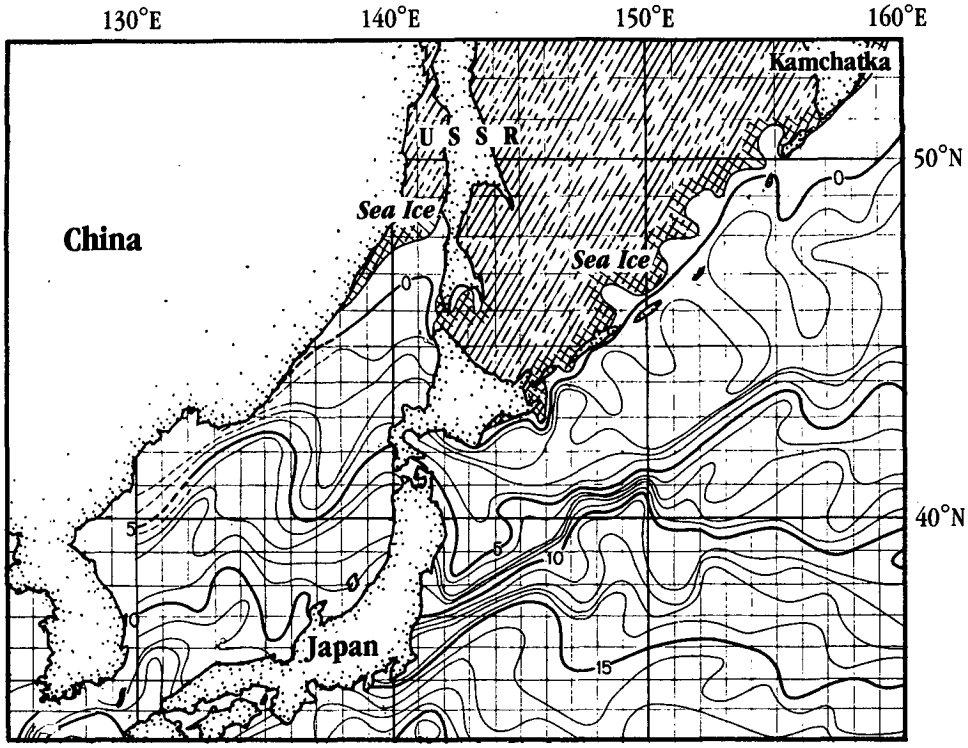

FIG. 10. Sea surface temperatures for the Sea of Japan, 1–10 March 1978 (Japan Meteorological Agency).

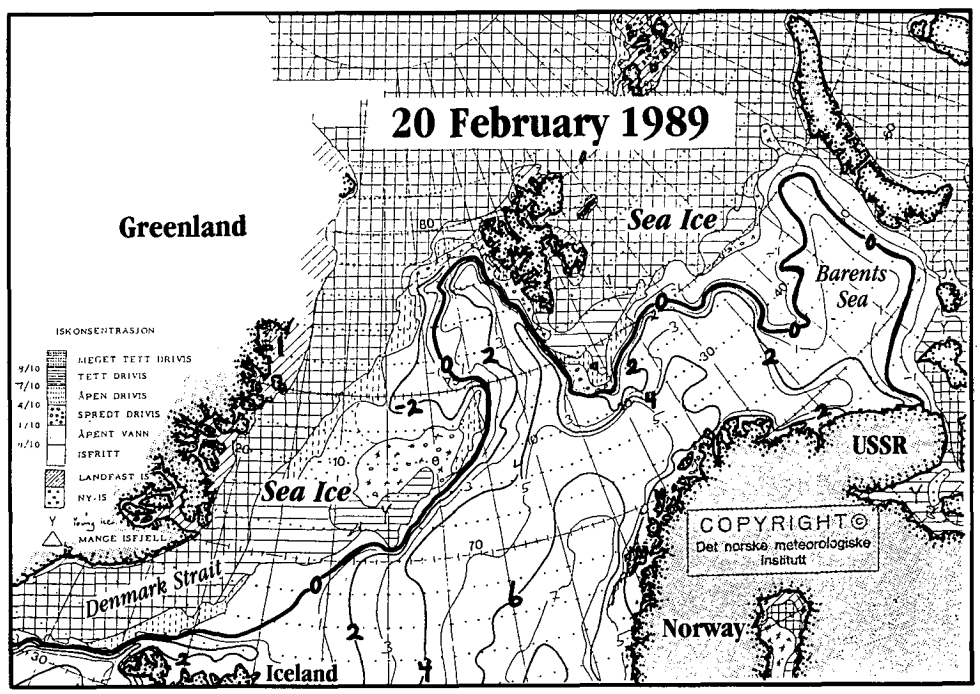

FIG. 11. Sea surface temperature for the Barents and Greenland seas, 20 February 1989 (Norwegian Meteorological Institute).

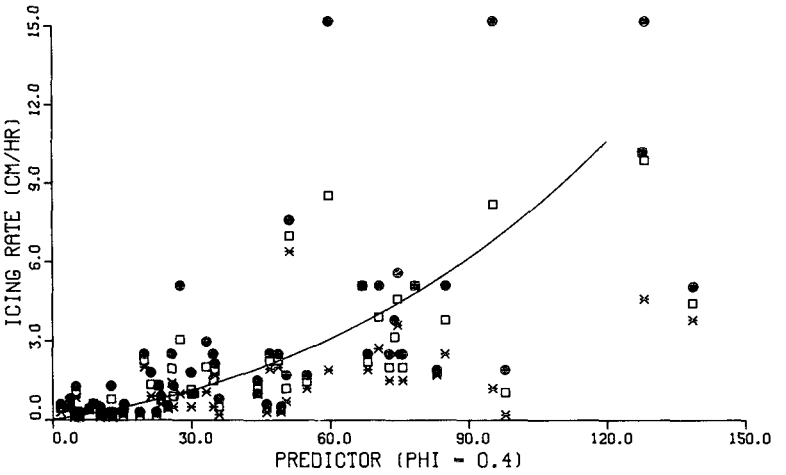

FIG. 12. Comparison of the NOAA algorithm with icing data (Pease and Comiskey 1985). Circles are maximum icing rate, crosses are event rate, and squares are the average of these rates, used in the development of the NOAA algorithm (OPPC).

(Table 2) and within an acceptable range of the original OPPC algorithm. More importantly, the new computed break points for the predictor value between icing classes are within 0.2 [or 1% of those from OPPC (Table 1)]. For the combined dataset, however, the best fit is for $\Phi = 0.3$ with $a_0 = 0.75$ (Table 3). Both a_0 scores show skill compared with $a_{901} = 0.46$ for 102 random data values. An updated algorithm is presented in Table 4, which now is derived from data spanning -1.8°C to 6.5°C. The results of the updated algorithm are plotted with the combined PC and ZLH datasets in Fig. 13. An important point is that the original algorithm is robust with regard to new observations. There is no impact in the sea-temperature range of the North Pacific and a minor change at low temperatures with inclusion of the ZLH data. In the original OPPC the sensitivity to the training dataset was rather flat between $\Phi = 0.3$ and 0.4. The sensitivity now has a distinct max at $\Phi = 0.3$.

The max a_0 score for all Φ for the second case based on event rates is 0.67. It is concluded that the development of OPPC was not sensitive to the extreme values in the PC dataset, a goal of the original analysis. ZLH pointed out that deterministic models have an uncertainty of a factor of 5 in the estimates of spray delivery based upon vessel type. This uncertainty is greater than the estimated uncertainty of <2–3 in the empirical/physical approach of OPPC. Based on ZLH observations from the cold sea-temperature Labrador Sea, both the magnitude of icing rates and functional form of the predictor from OPPC are consistent with eastern Canadian waters. The quality ZLH observation set contradicts the conclusion obtained from a lesser quality observation set (the Stallabrass set; Roebber and Mitten 1987) that OPPC may overpredict for this region.

TABLE 3. Predicted/observed table for the combined ZLH and PC observation set for icing categories defined by an updated icing algorithm (Table 4) with $\Phi = 0.3$. The number of correctly predicted observations is 76% or 75%.

	Observed		
Predicted	L	M	H
Heavy	2	8	24
Moderate	8	24	2
Light	28	5	1

6. Icing threshold versus vessel size

Icing forecasts provided by weather services provide the regional extent for potential icing based only on meteorological and oceanographic data and forecasts.

TABLE 4. Categorical forecast procedure based on the combined ZLH and PC observation sets. The data span a sea temperature range of -1.8°C to 6.5°C. The method shows skill based on comparison to random datasets (appendix in OPPC).

	Icing class			
	Light	Moderate	Heavy	Extreme
Icing rate (cm h^{-1})	<0.7	0.7–2.0	>2.0	
Predictor (PPR*) (m°C s^{-1})	<22.4	22.4–53.3	>53.3	>83.

* $PPR = V_a(T_f - T_a)[1 + 0.3(T_w - T_f)]^{-1}$

where

V_a wind speed (m s^{-1})
T_f freezing point of seawater (-1.8°C)
T_a air temperature (°C)
T_w sea temperature (°C)

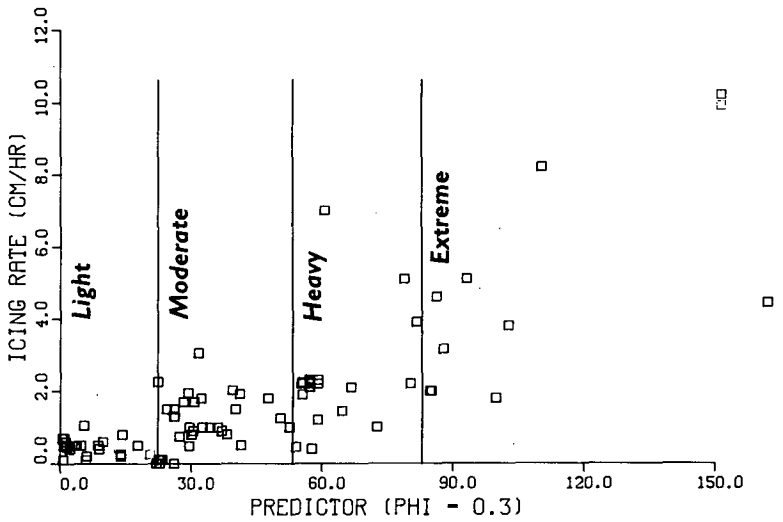

FIG. 13. Comparison of the results of the revised icing algorithm (Table 4) with the combined spray icing datasets from Alaskan and Labrador Sea waters.

However, for ship-specific forecasts, vessel length versus wavelength and height is an important factor. This section discusses vessel length as an auxiliary factor of relevance to individual vessel operators and planning purposes. It also may be a starting point for more sophisticated models of mass flux onto a vessel than Zakrzewski et al. (1988b) or Horjen and Carstens (1989). There is presently no theory that can be used to estimate spray-liquid water content and its vertical variation under various wave impact conditions (Makkonen 1989).

For small fishing vessels (20 m) proceeding into waves at typical speeds the wind speed for moderate icing is sufficient to provide spray to forward deck areas. For large trawlers (50 m), coastal freighters (75–150 m), and military vessels there is a threshold wave height in addition to the necessary heat flux. Sawada (1966) reports a threshold wave height of 2.5 m for icing; this is equivalent to 10.0-m s^{-1} wind for 200-km fetch. Zakrzewski (1987) reports a threshold wind velocity of 10 m s^{-1} for 40-m Soviet MFV-type vessels. This section suggests a spray generation threshold as a function of length based on seakeeping theory. Note, however, that seakeeping depends on individual ship characteristics and vessel speed.

When the heave and pitch of a vessel is large, spray

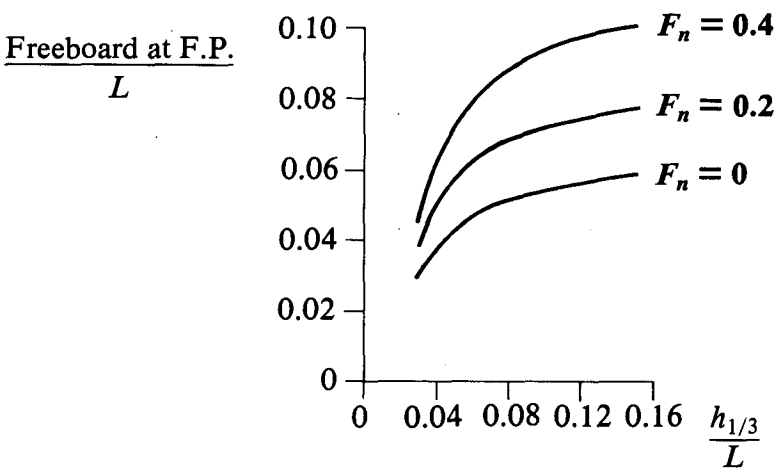

FIG. 14. The limit on nondimensional forward speed to avoid 1 in 20 wave overtoppings of the vessel as a function of freeboard and significant wave height (from Price and Bishop 1974).

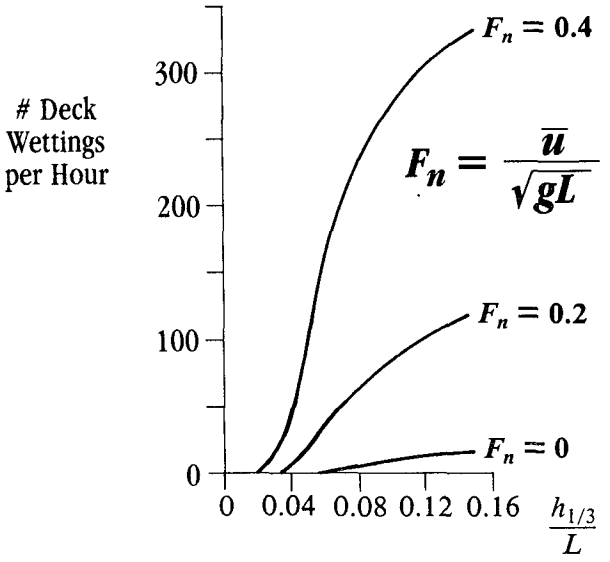

FIG. 15. Expected number of deck wettings/h as a function of significant wave height and vessel speed (from Price and Bishop 1974). A 0.04 significant wave height/length ratio is adopted for the beginning of significant spray delivery.

is generated by the interaction of the vessel and the wave field.[1] Linear-response analysis is successful for estimating heave and pitch of a vessel forced by an ocean-wave spectrum (St. Denis and Pierson 1953)

$$\left.\begin{aligned}\Phi_{\theta\theta}(\omega_e) &= |H_{\theta\zeta}(\omega_e)|^2\Phi_{\zeta\zeta}(\omega_e)\\ \Phi_{zz}(\omega_e) &= |H_{z\zeta}(\omega_e)|^2\Phi_{\zeta\zeta}(\omega_e)\end{aligned}\right\} \quad (4)$$

Here $H_{\theta\zeta}$ and $H_{z\zeta}$ are the response functions that relate pitch θ and heave z spectra to the ocean wave spectrum $\phi_{\zeta\zeta}$. It is important to consider a range of wave frequencies (thus the use of a spectral representation) because a ship is expected to have large motions and thus a large response function, only for a certain range of wave frequencies. Because of the ship's forward motion, the ship responds to the Doppler shifted wave frequency, the encounter frequency, ω_e:

$$\omega_e = \omega - \frac{\omega^2}{g}\bar{U}\cos\gamma \quad (5)$$

[1] Heave of a vessel is the vertical displacement of the center of mass of the vessel and pitch is the forward rotation about this center.

For the present purpose, one can make use of the results from seakeeping theory, referring the derivation details to their principal sources. With the assumption that a ship responds hydrostatically to waves and that wave spectra can be scaled by the significant wave height, the rms of pitch and heave has been determined as a function of nondimensional ship speed, the vessel Froude number: $F_n = \bar{U}(gL)^{-1/2}$ (Price and Bishop 1974). Deck wetness due to shipping water occurs when the relative displacement between the ship and sea surface exceeds local freeboard

$$z_b(t) = z(t) + 0.5L\theta(t) - \zeta(t). \quad (6)$$

If the relative displacement of the bow is a narrow-banded process described by a Rayleigh probability function, the expected number of deck wettings per unit time is

$$N^H = \frac{1}{2\pi}\left(\frac{m_2}{m_0}\right)^{1/2}\exp(-h^2/m_0). \quad (7)$$

For vessels steaming directly into waves, Fig. 14 gives the limits on non-dimensional forward speed to avoid more than 1 in 20 waves overtopping the deck as a function of significant wave height and freeboard. For example, a 100-m ship with a 7-m freeboard can expect wetting > 5% of the time when traveling >9.5 m s^{-1} (F_n = 0.3) in a sea of 6-m significant wave height. Figure 15 gives the number of wetness events per hour for a ship of freeboard/length ratio of 0.065. For all freeboards the onset of wetness occurs near a $h_{1/3}/L$ ratio of 0.04. For larger freeboard/length ratios, expected wetness is a strong function of forward speed.

Spray onto decks and superstructures required for heavy icing is probably fully developed at the 5% wetness criteria. With this assumption, a $h_{1/3}/L$ ratio of 0.04 provides the wind speed threshold for icing as a function of vessel length (Table 5). The bottom row indicates for winter conditions on the Bering Sea that the likelihood of encountering heavy icing conditions is small only for vessels > 150 m. Light icing by definition can occur for any vessel length because it requires only the necessary thermodynamic conditions.

Figure 16 plots observed wind speed versus vessel length from the PC Alaskan dataset. No cases were obtained with a wind speed < 8 m s^{-1}, i.e., no icing cases were obtained at low wind speeds and very low air temperatures. There is, perhaps, a wind speed threshold for vessels > 60 m.

TABLE 5. Calculated threshold wind speeds resulting in icing of ships of various lengths.

Parameter	Value					
Vessel length (m)	15	30	50	75	100	150
Significant wave height (m)	0.6	1.2	2.0	3.0	4.0	6.0
Wind speed (m s^{-1}) at 200-km fetch	5.0	7.4	9.8	12.5	15.0	20.0
Percent of observations with this wind speed or greater for Bering Sea in February (Brower et al. 1977)	83	69	47	27	15	4

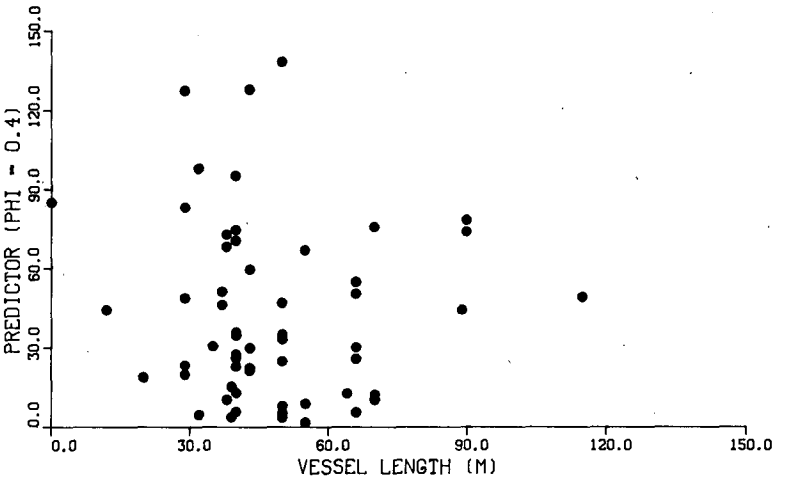

FIG. 16. Vessel length versus potential icing rate for the Pease and Comiskey (1985) dataset. Vessels < 70 m in length have encountered icing for the entire range of the environmental predictor from OPPC.

7. Summary and recommendations

Forecasts by weather services have the limitation that they must be regional and cannot be vessel specific. Forecasts should be easily communicated and understood, and should reflect the uncertainty in absolute rates both from the input data and the variation between vessels. For example, heavy icing should imply the likelihood that all but the largest vessels should take evasive action. Light icing may freeze deck gear and limit or curtail operations. It is important for weather services to standardize icing categories—light, moderate, or heavy—or any continuous algorithm on the basis of the range of meteorological and oceanographic conditions with potential for icing, with reference to one or two typical vessel types. Operational forecasts can then be made relative to the meteorological conditions without regard to ship-dependent variables. It is recommended that the World Meteorological Organization (WMO) develop such a standardization.

There have been improvements in deterministic modeling of the icing process since OPPC, most noticeably the influence of salinity (Makkonen 1987; Zakrzewski et al. 1988a). Operational application of these models is limited by the least well-modeled component, which is perhaps generation of spray, or water and airflow over the vessel (Makkonen 1989). Different models provide different quantitative results and sensitivities to input parameters (Zakrzewski et al. 1989). Historic (OPPC) and direct (ZLH) observations are required for first-order calibration of model predictions. Empiricism still remains a central part of forecast technique.

From the evidence presented there is no compelling reason to make changes in the current NOAA icing product. It provided quality guidance during the worst icing episode in the western Arctic in more than a decade and was shown to be robust over a sea-temperature range of −1.8° to 6.5°C when compared with an independent observation set (ZLH) and selected definition changes in the PC observation set. There is no evidence to change the magnitudes of potential icing rates for the definition of icing classes for typical large trawlers. In fact, the new observations (ZLH) support the icing rate definitions in OPPC over the previous "Stallabrass" eastern Canadian observation set.

Expansion from an Alaskan to a hemispheric product is under development (D. Feit, personal communication). For a new application, particularly to cold sea temperatures, the slightly modified algorithm (Table 5) is recommended over Table 1. Numerical guidance must be supported by experienced marine forecasters who recognize, perhaps, a rare cold-air advection icing event from all data sources. Anchorage Weather Service forecasters provided such timely information during January 1989. Vessel operators have the responsibility for interpretation of forecasts for their vessel.

Acknowledgments. This paper is Contribution No. 1104 from NOAA's Pacific Marine Environmental Laboratory to the Marine Services Project at PMEL. I have enjoyed discussions with D. Feit, G. Hufford, C. Pease, and R. Scheidt. R. Brown, P. Zakrzewski, and the reviewers provided particularly useful comments on the manuscript.

APPENDIX

Notation

V_a	wind speed
T_f	freezing point of seawater

T_w	sea temperature
T_a	air temperature
dH_i/dt	icing rate
dH_w/dt	supply of seawater spray
F	accretion fraction; ice growth/water delivered $(\rho_i dH_i/dt)(\rho_w dH_w/dt)^{-1}$
Φ	$\approx C_w L_i^{-1} F^{-1}$
A	$\approx C_H \rho_a C_a \rho_i^{-1} L_i^{-1}$
ρ_a, ρ_i	density of air and vessel icing
C_w, C_a	specific heat of seawater and dry air
L_i	latent heat of freezing for spongy sea ice
C_H	transfer coefficient for heat flux
$\Phi_{\theta\theta}$, Φ_{zz}, $\Phi_{\zeta\zeta}$	frequency spectrum for pitch, heave and waves
ω_e, ω	encounter frequency, wave frequency
$\bar{U}$	ship speed
γ	angle between ship heading and seaway
F_n	ship Froude number $\bar{U}(gL)^{-1/2}$
g	gravity
L	ship length
z_b	relative displacement of vessel and sea at the bow
h	ship freeboard
m_0	mean square vessel vertical displacement
m_2	mean square vessel vertical velocity
$h_{1/3}$	significant wave height

REFERENCES

Alden, R. F. 1988. Evaluation of FNOC/NMC/ECMWF atmospheric prediction model forty-eight hour forecast performance based on measures of synoptic similarity for April 1988. Office of Ocean Services, NOAA, Monterey, California (available from NOAA Library, 7600 Sand Point Way NE, Seattle, WA, 98115), 137 pp.

Bonner, W. D. 1988. Recent progress and future plans for numerical weather prediction at the National Meteorological Center. In: *Preprints 8th Conference on Numerical Weather Prediction,* American Meteorological Society, February 22–26, 1988, Baltimore, Md. J26–J33.

Brower, W. A., H. F. Diaz, A. S. Prechtel, H. W. Searby and J. L. Wise. 1977. Climate Atlas of the Outer Continental Shelf Waters and Coastal Regions of Alaska, Volume II, Bering Sea. AEIDC, Anchorage, Alaska. 443 pp.

De Angelis, R. M. 1974. Superstructure icing. *Mar. Wea. Log* **18:** 1–7.

Feit, D. M. 1987. Forecasting of superstructure icing for Alaskan waters. *Natl. Wea. Dig.* **12:** 5–10.

George, D. J. 1975. The frequency of weather conditions favourable for ship spray icing on the seas round Iceland during the 1972–73 winter. *Mar. Obs.* **45:** 177–185.

Horjen, I., and T. Carstens. 1989. Numerical modeling of sea spray icing on vessels. In: Proceedings 10th International Conference on Port and Ocean Engineering Under Arctic Conditions, June 1989, Luleå, Sweden, 694–704.

Lee, A. 1958. Ice accumulation on trawlers in the Barents Sea. *Mar. Obs.* **28:** 138–142.

McClain, E. P., W. G. Pichel and C. C. Walton. 1985. Comparative performance of AVHRR-based multichannel sea surface temperatures. *J. Geophys. Res.* **90:** 11 587–11 601.

Makkonen, L. 1987. Salinity and growth rate of ice formed by sea spray. *Cold Regions Sci. Tech.* **14:** 163–171.

——. 1988. Formation of spray ice on offshore structures. 9th International Symposium on Ice, Sapporo, Japan, 23–27 August, 1988.

——. 1989. Formation of spray ice on offshore structures. In: *Working Group on Ice Forces, 4th State-of the Art Report, CRREL Special Report 89-5,* Hanover, New Hampshire, 277–309.

Mertins, H. O. 1968. Icing on fishing vessels due to spray. *Mar. Obs.* **38:** 128–130.

Overland, J. E., C. H. Pease, R. W. Preisendorfer and A. L. Comiskey. 1986. Prediction of vessel icing. *J. Climate and Applied Meteor.* **25:** 1793–1806.

Pease, C. H., and A. L. Comiskey. 1985. Vessel icing in Alaskan waters. NOAA Data Rep., ERL PMEL-14, Pacific Marine Environmental Laboratory, Seattle, 16 pp. (NTIS No. PB86-164662)

Price, W. G., and R. E. D. Bishop. 1974. *Probabilistic Theory of Ship Design.* New York: J. Wiley and Sons, 311 pp.

Roebber, P., and P. Mitten. 1987. Modeling and measurement of icing in Canadian waters. Canadian Climate Center Report 87–15, Downsview, Ontario, Canada. unpublished manuscript, 150 pp. (available from the NOAA Library, 7600 Sand Point Way NE, Seattle, WA 98115).

St. Denis, M., and W. J. Pierson, Jr. 1953. On the motion of ships in confused seas. *Transactions, Soc. Naval Architects and Marine Engineers* **61:** 280–357.

Sawada, T. 1966. A forecasting method for ship icing near the Kuril Islands. *J. Meteor. Res.* **18:** 665–673.

Stallabrass, J. R. 1971. Meteorological and oceanographic aspects of trawler icing of the Canadian east coast. *Marine Observer* **41:** 107–121.

——. 1980. Trawler icing: A compilation of work done at N.R.C. Mech. Eng. Rep. MD-56, N.R.C. No. 19372, National Research Council, Ottawa, Canada, 103 pp.

Walton, C. C. 1988. Nonlinear multichannel algorithms for estimating sea surface temperature with AVHRR satellite data. *J. Applied Meteor.* **27:** 115–124.

Zahn, P. 1985. Four recent encounters with topside icing. Proceedings of 1985 U.S. Navy Symposium on Arctic/Cold Weather Operations of Surface Ships, 3–5 December 1985, 123–148.

Zakrzewski, W. P. 1987. Splashing a ship with collision-generated spray. *Cold Regions Science and Technology,* **14:** 65–83.

——, and E. P. Lozowski. 1987. The application of a vessel spraying model for predicting ice growth rates and ice loads on a ship. In: Proceedings 9th International Conf. on Port and Ocean Engineering Under Arctic Conditions, September, 1987, Fairbanks, Alaska.

——, R. Blackmore and E. P. Lozowski. 1988a. Mapping the ice growth rates on sea-going ships. *J. Meteor. Soc. Japan* **66:** 661–675.

——, E. P. Lozowski and R. Z. Blackmore. 1988b. The use of a ship spraying/icing model to estimate the effect of the direct spray flux on the icing rate. Proceedings of the 7th International Workshop on Atmospheric Icing of Structures, Sept. 6–9, 1988. Paris, France.

——, —— and I. Horjen. 1989. The use of ship icing models for forecasting icing rates on sea-going ships. In: Proceedings 10th International Conf. on Port and Ocean Engineering Under Arctic Conditions, June 1989, Luleå, Sweden.